Classical image treatment of a geometry composed of a circular conductor partially merged in a dielectric cylinder and related problems in electrostatics

2005 J. Phys. A: Math. Gen. 38 6253

(http://iopscience.iop.org/0305-4470/38/27/011)

INSTITUTE OF PHYSICS PUBLISHING JOURNAL OF PHYSICS A: MATHEMATICAL AND GENERAL

J. Phys. A: Math. Gen. **38** (2005) 6253–6269 doi:10.1088/0305-4470/38/27/011

Classical image treatment of a geometry composed of a circular conductor partially merged in a dielectric cylinder and related problems in electrostatics

D Palaniappan

Texas A&M University at Qatar, c/o Qatar Foundation, PO Box 5825, Doha, Qatar

Received 21 March 2005, in final form 24 May 2005
Published 22 June 2005
Online at stacks.iop.org/JPhysA/38/6253

Abstract

The classical treatment of the Laplace equation by electrical inversion is used to obtain analytical expressions for the two-dimensional perturbed electrostatic fields in the presence of a two-phase 2D object. The geometry of the two-phase object is composed of two overlapping infinitely long cylinders C_a and C_b of radii a and b, respectively, intersecting at a vertex angle $\frac{\pi}{2}$. The composite inclusion has the shape resembling a 2D *snowman* type of object with a conducting cylinder C_a partly protruded into the dielectric cylinder C_b with a dielectric constant different from that of the host medium. The mathematical problem with this inclusion in the electrostatic environment is formulated in terms of electric potentials (and complex potentials as well) with the mixed Dirichlet and Neumann boundary conditions at the boundary of the hybrid object. General expressions for the perturbed electrostatic fields in the two phases are obtained in a straightforward fashion using Kelvin's inversion together with shift and reflection properties of harmonic functions. The general results are exploited to derive solutions for the hybrid object embedded in (i) a transverse or a longitudinal uniform field and (ii) a field generated by a dipole. The dipole coefficients are extracted directly from the exact solutions in a fairly simple manner. The plots of the normalized polarizabilities (derived from dipole coefficients) for the imposed uniform field show that the polarizability in the longitudinal direction is greater or less than the transverse polarizability depending on the dielectric constants of the composite body and the host medium. The equipotential plots generated using the exact solutions also show fascinating field patterns. An interesting connection between the present solutions and the cyclic groups in abstract algebra is outlined as well in the appendix.

PACS number: 41.20.Cv

1. Introduction

One of the oldest yet most powerful methods of solving boundary value problems in electrostatics is the method of inversion. This technique, widely known as the classical method of images, was introduced by Sir William Thomson (later known as Lord Kelvin) in 1845 [1] and has been used successfully to solve a variety of problems in electrostatics [2–5], in hydrodynamics [6, 7], in elastostatics [8] and even in low-frequency scattering [9, 10]. The basic idea of the method is to find the fictitious images whose field, combined with the field generated by the sources, gives rise to some desired boundary condition. For a conductor, the condition is that the boundary be an equipotential surface. For a dielectric, the boundary condition is that both the potential and flux be continuous across the surface. An explicit formula for the image of a charge in a cylindrical conductor or in a dielectric cylinder is well known, as is the formula for the image of a charge in a spherical conductor. The corresponding rule for the image of a charge in a non-circular (such as ellipse, for instance) or in a nonspherical (such as a spheroid, an ellipsoid, etc) geometry becomes somewhat complicated and a simple formula does not seem to exist.

The essential constituents involved in the classical method of images are

- the image point and its location in a specific geometry;
- suitable image singularities such as charges, dipoles, etc;
- strengths of the image singularities in order to satisfy the desired boundary conditions.

Lord Kelvin used this so-called image principle to solve static problems involving a perfectly electrically conducting (PEC) grounded sphere. Kelvin's image principle also has its two-dimensional counterpart which originally was developed in the context of hydrodynamics [6] and later extended to electrostatics [11]. The use of the method of images to half-space electrostatic problems is also well known [3]. In spite of the basic limitation to statics, the method of inversion is applicable to time-harmonic problems, even at microwave frequencies. This requires that the region of interest be small enough in wavelengths, what is known as quasi-static approximation. In this case, the medium parameters are not the static ones but those taken at the frequency in question, in general, with complex values.

Spheres, cylinders and half-spaces belong to the class of objects for which the image principle works pretty well in many circumstances. A natural question arises whether the image principle can be used for body profiles other than spheres, cylinders and half-spaces. It turns out that for complex body shapes the image principle becomes extremely difficult to apply and requires quite a lot of guesswork and iterative adjustments in order to obtain even approximate solutions. Recently [12, 13], it was shown that Kelvin's inversion, whose applicability has been long thought restricted to problems involving spheres, could actually be used to determine exact solution of a variety of problems involving overlapping spheres and cylinders. This idea is well suited especially for a class of boundary value problems involving merging (intersecting) surfaces. The surfaces that belong to the category of merging objects can be modelled, for instance, as two spheres or two infinitely long circular cylinders (such as considered in this paper) intersecting at a vertex angle. Such surfaces are not without practical interest. The merging spheres/cylinders under study might for example be biological cells, metal–insulator composites, rocks, etc. Furthermore, these surfaces depart from spherical/circular shape and the fact that exact solutions can be found for problems involving these surfaces make them members of a very exclusive family.

Although the image method works well for conducting overlapping spheres [2, 5, 12] and cylinders [13], it does not offer sufficient clues for electrostatic problems involving dielectric intersecting cylinders and spheres. The use of bicylindrical (for merging cylinders) and

toroidal (for merging spheres) coordinates might be an alternative approach [14, 15] but these methods do not lend themselves to solutions in a form suitable for further calculations including the computation of multiparticle interactions. Moreover, in these special coordinate frames, the boundary conditions result in differential equations rather than the algebraic equations for the unknown coefficients which are, in general, difficult to deal with [16]. Here, we make an attempt to solve a basic electrostatic problem for a special nontrivial geometry of 2D *snowman type*. More specifically, we consider a geometry consisting of a conducting cylinder partially merged in a dielectric cylinder with a dielectric constant different from that of the surrounding host medium and construct solutions for the electrostatic potentials using the classical image principle. It is assumed that the angle of intersection of the two cylindrical surfaces of the two-phase object is $\frac{\pi}{2}$. This assumption allows the two bounding circles to share a common inverse point, a requirement that is *crucial* for the exact analysis. The exterior boundary value problem for the determination of the electric potentials is solved analytically and general solutions representing a set of basis functions are provided in terms of the basic unbounded potential. The solutions are expressed in terms of Green functions for specific externally imposed fields. The advantage of these forms of solutions is that various physical quantities of interest can be computed directly. Furthermore, these closed-form solutions provide results which, beside their significance to electrostatic theory, can be used to validate numerical codes designed to handle objects of more general shapes [17]. Although the application of the results are presented in the context of electrostatics, they can indeed be utilized in thermal conduction problems as well.

The paper is organized as follows. In section 2, the geometry of the two-phase 2D object and some geometrical relationships relevant in the present contexts are discussed. The formulation of the problem is done in section 3 both in Cartesian and complex frames. The solution method, the general solutions in the form of a theorem and solutions to other related problems in electrostatics all appear in section 4. Some illustrative examples and related details are given in section 5. The main findings of the present work and other comments are provided in section 6. Finally, in the appendix, the connection of our results to cyclic groups in abstract algebra is discussed.

2. Geometry of the heterogeneous two-phase cylindrical object Γ

The two-phase double cylindrical snowman-type geometry of the heterogeneous object is depicted in figure 1. This geometry is composed of two unequal overlapping infinitely long circular cylinders C_a and C_b of radii a and b with centres O and O', respectively. It is assumed that the two cylinders intersect orthogonally. The boundary of the heterogeneous body is denoted by $\Gamma = C_a \cup C_b$, where C_a is the circle with $r = a$ and C_b is part of the circle where $r' = b$. The origin of the coordinate system is chosen at the centre of the circle C_a. Since the circles overlap at a contact angle $\pi/2$, the two centres share a common inverse point D. In the right-angled triangle OAO', $c^2 = a^2 + b^2$, where $OO' = c$ is the centre-to-centre distance between the two circles. As shown in figure 1, the line AB intersects OO' at D. Hence, $OD = a^2/c$ and $DO' = b^2/c$. It follows that

$$\frac{1}{(OA)^2} + \frac{1}{(O'A)^2} = \frac{1}{(DA)^2}, \tag{1}$$

which is an interesting geometrical relation connecting the radii of the two circles and the distance between the inverse point D and the vertex A. Let (r, θ), (r', θ') and (R, Θ) be the polar coordinates of any point outside the assembly Γ with O, O' and D as origins, respectively, and let z, z' and Z be the corresponding complex positions. The following geometrical relations

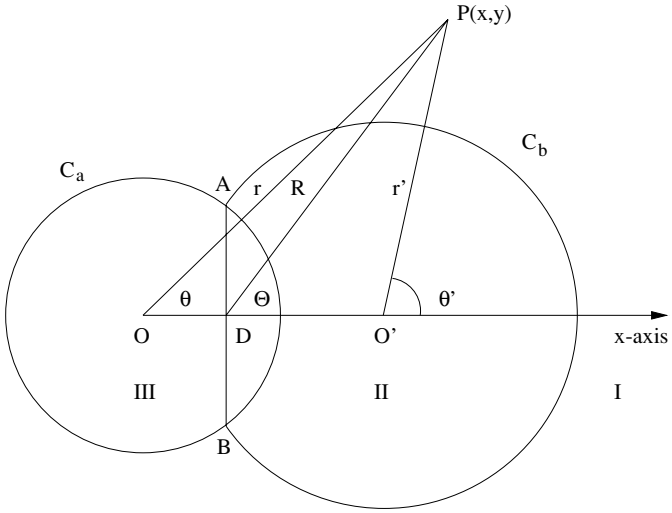

Figure 1. Schematic of a heterogeneous two-phase cylindrical snowman-type object Γ.

are clear from figure 1:

$$r^2 = r'^2 + 2cr'\cos\theta' + c^2, \tag{2}$$

$$r'^2 = r^2 - 2cr\cos\theta + c^2, \tag{3}$$

$$R^2 = r^2 - 2\frac{a^2}{c}r\cos\theta + \frac{a^4}{c^2} = r'^2 + 2\frac{b^2}{c}r'\cos\theta' + \frac{b^4}{c^2}. \tag{4}$$

It follows from (2)–(4) that on the circles C_a and C_b, r' and r reduce to

$$r' = \frac{c}{a}R, \qquad \text{on} \quad r = a, \tag{5}$$

$$r = \frac{c}{b}R, \qquad \text{on} \quad r' = b. \tag{6}$$

The useful geometrical relations in the complex plane are

$$z = z' + c = Z + \frac{a^2}{c}, \qquad Z = z' + \frac{b^2}{c}, \qquad c^2 = a^2 + b^2.$$

Also, we have

$$c^2 Z\bar{Z} = \begin{cases} a^2 z'\bar{z}', & \text{on} \quad |z| = a, \\ b^2 z\bar{z}, & \text{on} \quad |z'| = b. \end{cases}$$

The cylindrical region C_b is filled with a dielectric with a constant different from that of the host medium and the cylinder C_a is a perfect conductor. The medium exterior to Γ is designated as I and the cylindrical regions C_b and C_a as II and III, respectively.

3. Formulation

Consider a stationary two-phase cylindrical geometry Γ embedded in an arbitrary two-dimensional electrostatic field. Let $k^{(\mathrm{I})}$ be the dielectric constant of the medium outside

Γ and $k^{(\mathrm{II})}$ be the dielectric strength for phase II of the cylinder C_b (figure 1), respectively. The electric potential outside Γ is denoted by $\phi^{(\mathrm{I})}(x, y)$ and the potential inside the dielectric phase by $\phi^{(\mathrm{II})}(x, y)$. It is well known that the electric potentials satisfy the 2D Laplace equation which is

$$\nabla^2\phi^{(\mathrm{I})} = 0 = \nabla^2\phi^{(\mathrm{II})}, \qquad \nabla^2 = \frac{\partial^2}{\partial x^2} + \frac{\partial^2}{\partial y^2} \tag{7}$$

in the respective phases. The boundary conditions for the electric potentials at the interfaces are

- zero potential (Dirichlet boundary condition) on the conducting surface C_a;
- continuity of the potential across the dielectric phase C_b;
- continuity of the flux across the dielectric phase C_b.

In mathematical terms, the above conditions read

$$\phi^{(\mathrm{I})} = 0, \qquad \text{on} \quad r = a, \tag{8}$$

$$\phi^{(\mathrm{I})}(x, y) = \phi^{(\mathrm{II})}(x, y), \qquad \text{on} \quad r' = b, \tag{9}$$

$$k^{(\mathrm{I})}\frac{\partial\phi^{(\mathrm{I})}}{\partial r'} = k^{(\mathrm{II})}\frac{\partial\phi^{(\mathrm{II})}}{\partial r'}, \qquad \text{on} \quad r' = b, \tag{10}$$

$$\phi^{(\mathrm{II})} = 0, \qquad \text{on} \quad r = a. \tag{11}$$

On the conducting and dielectric interfaces, respectively. Note that the heterogeneous inclusion leads to the mixed Dirichlet- and Neumann-type boundary conditions on the two-phase object of Γ. The equivalent boundary value problem in terms of complex potentials $W^{(\mathrm{I})}(z) = \phi^{(\mathrm{I})} + \mathrm{i}\psi^{(\mathrm{I})}$ in the continuous phase and $W^{(\mathrm{II})}(z) = \phi^{(\mathrm{II})} + \mathrm{i}\psi^{(\mathrm{II})}$ in the dielectric phase, respectively, is as follows:

$$\frac{\partial^2 W^{(\mathrm{I})}}{\partial z\partial\bar{z}} = 0, \qquad \frac{\partial^2 W^{(\mathrm{II})}}{\partial z\partial\bar{z}} = 0, \tag{12}$$

with the boundary conditions

$$\mathrm{Re}(W^{(\mathrm{I})}) = 0, \qquad \text{on} \quad |z| = a, \tag{13}$$

$$\mathrm{Re}(W^{(\mathrm{I})}) = \mathrm{Re}(W^{(\mathrm{II})}), \qquad \text{on} \quad |z'| = b, \tag{14}$$

$$k^{(\mathrm{I})}\,\mathrm{Re}\left[z'\frac{\partial W^{(\mathrm{I})}}{\partial z'} + \bar{z}'\frac{\partial W^{(\mathrm{I})}}{\partial\bar{z}'}\right] = k^{(\mathrm{II})}\,\mathrm{Re}\left[z'\frac{\partial W^{(\mathrm{II})}}{\partial z'} + \bar{z}'\frac{\partial W^{(\mathrm{II})}}{\partial\bar{z}'}\right], \qquad \text{on} \quad |z'| = b, \tag{15}$$

$$\mathrm{Re}(W^{(\mathrm{II})}) = 0, \qquad \text{on} \quad |z| = a. \tag{16}$$

Below, we outline a method of solving the above boundary value problem for the electric/complex potential using the classical method of images.

4. The method and general solutions

Our main goal here is to describe a technique to solve the boundary value problem formulated in the previous section. Although, the mixed boundary conditions at the interfaces make the problem somewhat complicated, the idea of classical method of images offers a clue to resolve the technical difficulties for this nontrivial geometry. Since the images of an unbounded arbitrary electrostatic field in a conducting and dielectric cylinders are quite well known, we use them here to obtain the solutions for the underlying boundary value problem for the geometry Γ. This is achieved by taking continuous reflections of the images, in the usual

manner, and it turns out that this process leads to exact solutions after three steps. The essential steps involved in the derivation of the general solutions may be described as follows:

Step 1. Reflect a given electrostatic field ϕ_0 on the conducting circular cylinder C_a and call the perturbation field as ϕ_a.

Step 2. Reflect the given electrostatic field ϕ_0 on the dielectric cylinder C_b and call the perturbation to the given electrostatic field as $\phi_b^{(\mathrm{I})}$ and $\phi_b^{(\mathrm{II})}$, respectively.

Step 3. Reflect ϕ_a obtained in step 1 in cylinder C_b and call the perturbation to ϕ_a as $\phi_{ab}^{(\mathrm{I})}$ and $\phi_{ab}^{(\mathrm{II})}$. Reflecting $\phi_b^{(\mathrm{I})}$ and $\phi_b^{(\mathrm{II})}$ obtained in step 2 in sphere C_a will result in the same potentials, i.e. $\phi_{ab}^{(\mathrm{I})} = \phi_{ba}^{(\mathrm{I})}$ and $\phi_{ab}^{(\mathrm{II})} = \phi_{ba}^{(\mathrm{II})}$.

Therefore, the desired solutions are achieved in this fashion. For convenience, we use the two-dimensional Cartesian coordinates. Let (x, y), (x', y') and (X, Y) denote the Cartesian coordinates of a point $P(x, y)$ outside Γ with O, O' and D as origins, respectively. The Cartesian and polar coordinates are related by $x = r\cos\theta$ and $y = r\sin\theta$, with similar relations for the coordinates with respect to other origins. Since x does not appear explicitly in the Laplacian operator ∇^2, it is form invariant under translation origin along the x-axis. The following properties are true for equation (7):

(A) *Inversion.* If $\phi_0(x, y)$ is a solution of (7), then $\phi_0\left(\frac{a^2}{r^2}x, \frac{a^2}{r^2}y\right)$ is also a solution of (7), where a is the radius of inversion.

(B) *Reflection.* If $\phi_0(x, y)$ is a solution of (7), then $\phi_0(-x, y)$ is also a solution.

(C) *Translation of origin.* If $\phi_0(x, y)$ is a solution of (7), then $\phi_0(x + h, y)$, where h is a constant, is also a solution.

Note that (B) and (C) are also true for the corresponding operations with the y-coordinate. Below, the general expressions for the electrostatic fields in the two phases are presented in the form of a theorem followed by a simple proof. For the sake of completeness, the solutions in terms of complex variables for the two overlapping circles are also provided.

4.1. The theorem

Theorem 1. *Let $\phi_0(x, y)$ be the electric potential for the two-dimensional electrostatic field whose singularities (i.e., charges, dipoles, etc) lie outside a heterogeneous composite snowman-type geometry with the boundary Γ formed by two generally unequal circular surfaces intersecting orthogonally. When a composite object Γ is introduced in this two-dimensional electrostatic field, the modified electric potentials due to the heterogeneous cylindrical body in the respective phases I and II become*

$$\phi^{(\mathrm{I})}(x, y) = \phi_0(x, y) - \phi_0\left(\frac{a^2}{r^2}x, \frac{a^2}{r^2}y\right) - \frac{1-k}{1+k}\left[\phi_0\left(c + \frac{b^2}{r'^2}x', \frac{b^2}{r'^2}y'\right) - \phi_0\left(\frac{a^2}{c} - \frac{a^2b^2}{c^2R^2}X, \frac{a^2b^2}{c^2R^2}Y\right)\right] \tag{17}$$

for phase I and

$$\phi^{(\mathrm{II})}(x, y) = \frac{2k}{1+k}\left[\phi_0(x, y) - \phi_0\left(\frac{a^2}{r^2}x, \frac{a^2}{r^2}y\right)\right] \tag{18}$$

for phase II, where $k = \frac{k^{(\mathrm{I})}}{k^{(\mathrm{II})}}$.

Proof. By virtue of the properties (A), (B) and (C), $\phi^{(\mathrm{I})} - \phi_0$ (the perturbation terms in $\phi^{(\mathrm{I})}$ in equation (17)) and $\phi^{(\mathrm{II})}$ (given by equation (18)) are solutions of equation (7). By a

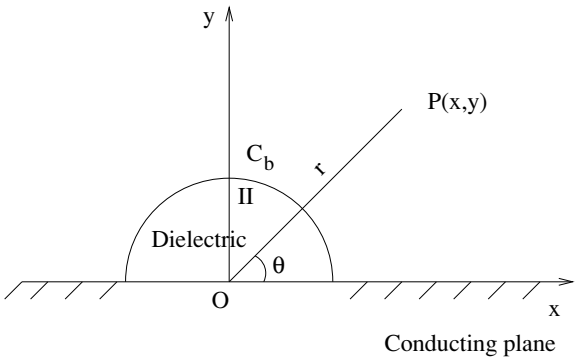

Figure 2. Schematic of a dielectric cylinder half buried in a conducting plane.

direct verification, it can be seen that $\phi^{(\mathrm{I})}$ and $\phi^{(\mathrm{II})}$ satisfy the boundary conditions (8)–(11). Since the singularities of ϕ_0 lie outside Γ, the singularities of the perturbation terms in $\phi^{(\mathrm{I})}$ will all lie inside Γ. Hence, the perturbed electric potential for phase I does not introduce new singularities outside Γ. Finally, since $\phi_0(x, y) = o(r)$ at the origin, the perturbation terms in (17) are at most of order $o\left(\frac{1}{r}\right)$ for large r. Therefore, the perturbation electric fields in phase I tend to zero as $r \to \infty$. This completes the proof. □

The expressions given in (17) and (18) represent the most general solutions of the electrostatic problem formulated in section 3. They can be used to construct solutions for various externally imposed electric potentials (in section 5, this is done for some representative cases). Furthermore, they can be used as a set of basis in the method of reflections approach for computing multiparticle interactions in electrostatic fields involving two-phase 2D objects.

The complex version of the solutions given in theorem 1 is as follows:

$$W^{(\mathrm{I})}(z) = F(z) - \bar{F}\left(\frac{a^2}{z}\right) + \frac{1-k}{1+k}\left[\bar{F}\left(c + \frac{b^2}{z'}\right) - F\left(\frac{a^2}{c} - \frac{a^2 b^2}{c^2 Z}\right)\right] \tag{19}$$

in the continuous phase I and

$$W^{(\mathrm{II})}(z) = \frac{2k}{1+k}\left[F(z) - \bar{F}\left(\frac{a^2}{z}\right)\right] \tag{20}$$

in the dielectric phase II. The real parts of the solutions (19) and (20) yield the electric potentials given in (17) and (18) in the respective phases. It may be pointed out that the imaginary parts of (19) and (20) also provide useful solutions especially in the context of hydrodynamics, where the current functions (Stokes stream functions) take a specific constant values (streamlines).

The method of images also yield solutions to other related electrostatic problems some of which are provided in the following subsection.

4.2. Solutions for related electrostatic problems

- *Dielectric cylinder of radius b half buried in a plane* $y = 0$. In this case (see figure 2), the potentials in the two phases are given by

$$\phi^{(\mathrm{I})}(x, y) = \phi_0(x, y) - \phi_0(x, -y) - \frac{1-k}{1+k}\left[\phi_0\left(\frac{b^2}{r^2}x, \frac{b^2}{r^2}y\right) - \phi_0\left(\frac{b^2}{r^2}x, -\frac{b^2}{r^2}y\right)\right] \tag{21}$$

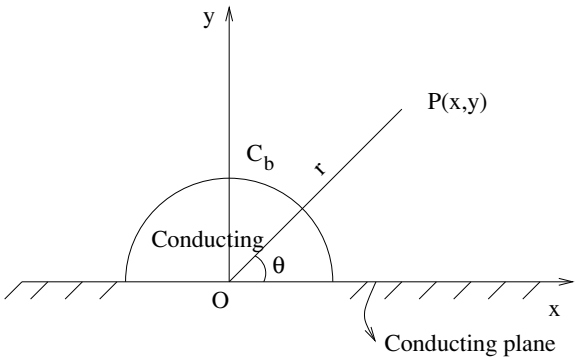

Figure 3. Schematic of a conducting cylinder half buried in a conducting plane.

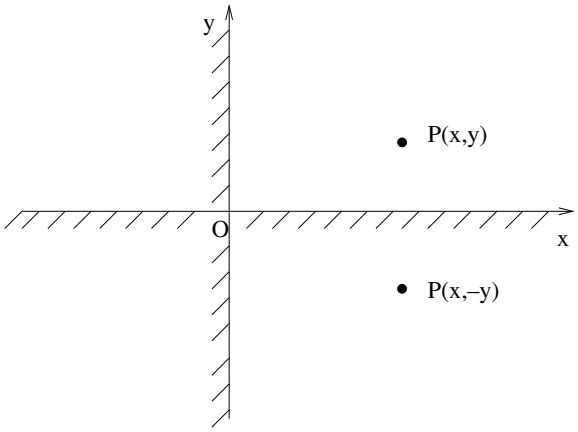

Figure 4. Schematic of two intersecting conducting planes.

for phase I and

$$\phi^{(\mathrm{II})}(x, y) = \frac{2k}{1+k}\left[\phi_0(x, y) - \phi_0(x, -y)\right] \tag{22}$$

for phase II.

- *Conducting cylinder of radius b half buried in a plane* $y = 0$. Here we have the electric potential in phase I alone (figure 3) which is

$$\phi(x, y) = \phi_0(x, y) - \phi_0\left(\frac{b^2}{r^2}x, \frac{b^2}{r^2}y\right) - \phi_0(x, -y) + \phi_0\left(\frac{b^2}{r^2}x, -\frac{b^2}{r^2}y\right). \tag{23}$$

- *Two conducting intersecting planes.* This is the two-dimensional analogue of the case considered by Maxwell [2]. The electric potential for this case (figure 4) is given by

$$\phi(x, y) = \phi_0(x, y) - \phi_0(x, -y) - \phi_0(-x, y) + \phi_0(-x, -y). \tag{24}$$

In the following section, we use the solutions (17) and (18) presented in theorem 1 to generate solutions for the heterogeneous inclusion Γ embedded in specific unbounded potentials.

5. Illustrative examples

As an illustration of the results (17) and (18), we now derive the explicit solutions for the two-phase cylindrical object embedded in uniform and dipole fields imposed externally.

5.1. The two-phase cylindrical object Γ *in a uniform field*

Consider the composite geometry Γ consisting of a conducting cylinder of radius a and a dielectric cylinder of radius b (a hybrid composite geometry) intersecting at an angle $\pi/2$ embedded in a uniform field. For the imposed field of strength E along the y-direction, that is along the transverse direction, the potentials in the two phases calculated using (17) and (18) are given by

$$\phi^{(\mathrm{I})}(x, y) = Ey\left[1 - \frac{a^2}{r^2} - \frac{1-k}{1+k}\left(\frac{b^2}{r'^2} - \frac{a^2b^2}{c^2R^2}\right)\right] \tag{25}$$

for the region outside Γ and

$$\phi^{(\mathrm{II})}(x, y) = \frac{2Ey}{1+k}\left[1 - \frac{a^2}{r^2}\right] \tag{26}$$

for the dielectric phase. The image system in phase I consists of dipoles at the points O, O' and D of strengths $-Ea^2$, $-E\frac{1-k}{1+k}b^2$ and $E\frac{1-k}{1+k}\frac{a^2b^2}{c^2}$, respectively. The plots of equipotentials are shown in figures 5(*a*)–(*d*) for two different values of k and radii. It may be noted that equipotential patterns in the vicinity of Γ changes significantly as we vary these parameters.

Since we have found the solution in terms of elementary functions, it is now straightforward to extract the various physical quantities of interest. One of the fundamental physical quantities in electrostatics is the polarizability which is determined by the dipole coefficient. From (25) the dipole coefficient α_{yy} is given by

$$\alpha_{yy} = -E\left[a^2 + \frac{1-k}{1+k}\left(b^2 - \frac{a^2b^2}{c^2}\right)\right]. \tag{27}$$

The dipole coefficient depends on the radii, centre-to-centre distance of the two circles and the ratio of the two dielectric constants in the respective phases. Figure 6(*a*) shows the plots of the dipole coefficient versus the radii ratio b/a for different values of k. As seen from this graph, the dipole coefficient decreases for increasing values of the radii ratio and the dielectric ratio as well. For all values of $k > 1$, the quantity α_{yy} decreases with b/a and becomes negative for larger values of the radii ratio. This phenomenon may be attributed to the heterogeneity of the inclusion Γ.

For the field along the x-direction, that is along the longitudinal direction, the solutions in the respective regions obtained using (17) and (18) are

$$\phi^{(\mathrm{I})}(x, y) = E\left[x - \frac{a^2}{r^2}x - \frac{1-k}{1+k}\left(\left(c + \frac{b^2}{r'^2}x'\right) - \left(\frac{a^2}{c} - \frac{a^2b^2}{c^2r_1^2}x_1\right)\right)\right] \tag{28}$$

for the region outside Γ and

$$\phi^{(\mathrm{II})}(x, y) = \frac{2E}{1+k}\left[x - \frac{a^2}{r^2}x\right] \tag{29}$$

for the dielectric phase. The image system for the potential outside Γ for the longitudinal case, as in transverse case, consists of dipoles at the points O, O' and D, respectively. In addition, there are constants in the expressions for the electric potentials which may be due to the geometrical asymmetry. The plots of equipotentials are shown in figure 7 for two different

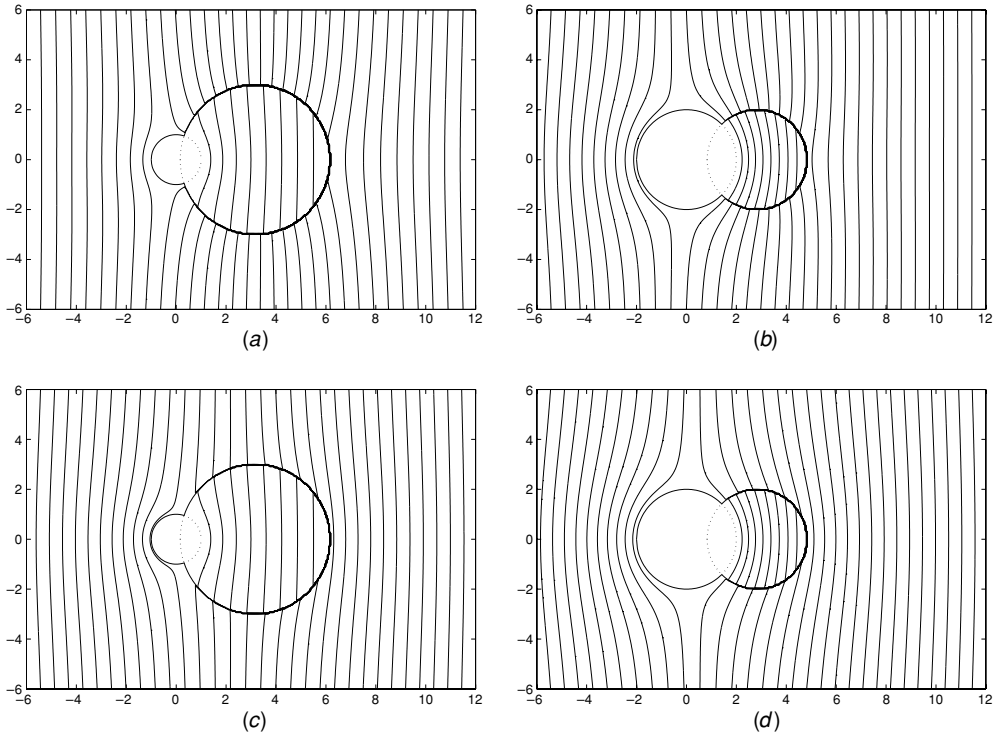

Figure 5. Equipotential plots for the uniform field along the transverse direction for different values of k and radii with $E = 1$. (i) $k = 0.5$: (*a*) $a = 1, b = 3$, (*b*) $a = 2, b = 2$; (ii) $k = 1.5$: (*c*) $a = 1, b = 3$, (*d*) $a = 2, b = 2$.

values of k and radii. It is evident from the figure that the equipotential patterns in the vicinity of Γ change for different values of k and the size of the composite geometry Γ.

The dipole coefficient extracted from (28) is given by

$$\alpha_{xx} = -E\left[a^2 + \frac{1-k}{1+k}\left(b^2 + \frac{a^2b^2}{c^2}\right)\right]. \tag{30}$$

As in the transverse case, the dipole coefficient α_{xx} for the longitudinal field depends on the geometry of the two-phase object and the ratio of the dielectric constants. The plots of the dipole coefficient are shown in figure 6(*b*). It is seen that the features of dipole coefficient α_{xx} are qualitatively similar to that of α_{yy}.

We can make a comparison between the two dipole coefficients given in (27) and (30). We first note that $\alpha_{xx} > \alpha_{yy}$ or $\alpha_{xx} < \alpha_{yy}$ according to $k < 1$ or $k > 1$ implying that the longitudinal polarizability is greater or less than the transverse polarizability depending on the ratio of the dielectric constants. This feature is seen explicitly in figure 6(*c*) where the two dipole coefficients are plotted for the sake of comparison. One can thus conclude that the ratio of the two dielectric constants of the two phases plays a crucial role on the two dipole coefficients and hence on the corresponding polarizabilities.

5.2. Field induced by a dipole located outside Γ

Consider a two-dimensional dipole of strength $p_1 = \mu_1$ placed outside Γ at $(-d, 0)$ with its axis parallel to the y-axis, that is, perpendicular to the line of centres (transverse dipole).

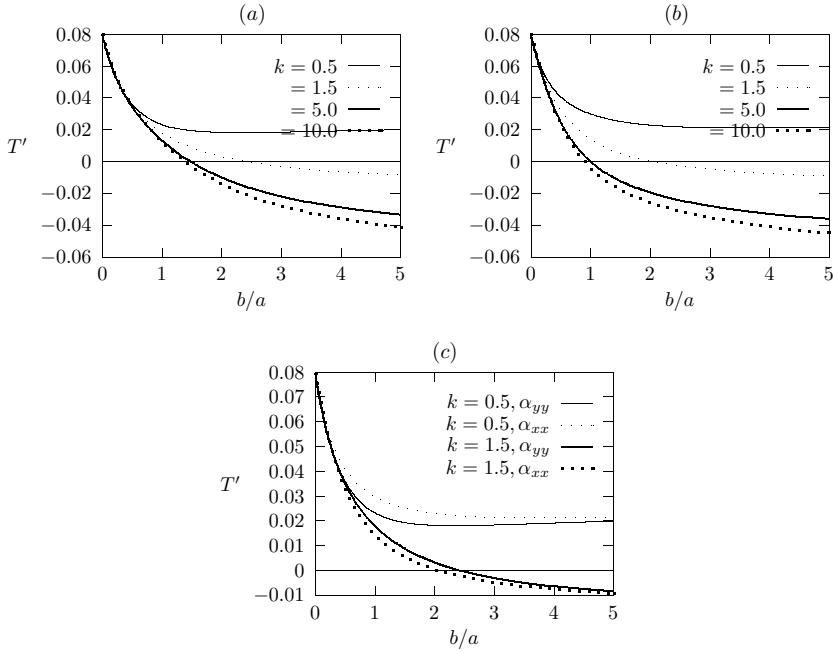

Figure 6. The dipole coefficient for uniform field along the x- and y-directions. Here T' is the normalized dipole coefficient.

Then,

$$\phi_0(x, y) = \mu_1 \frac{y_1}{R_1^3}, \tag{31}$$

where x_1 and y_1 are the Cartesian coordinates of a point P with D_1 (location of the initial singularity) as origin. The modified potential in phase I, using (17), becomes

$$\phi^{(\mathrm{I})}(x, y) = \mu_1 \left[\frac{y_1}{R_1^3} - \frac{a^2}{d^2} \frac{y_2}{R_2^3} + \frac{1-k}{1+k} \left(\frac{b^2}{(c+d)^2} \frac{y_3}{R_3^3} - \frac{(ab)^2}{(a^2+cd)^2} \frac{y_4}{R_4^3} \right) \right] \tag{32}$$

and the potential in phase II, using (18), is

$$\phi^{(\mathrm{II})}(x, y) = \frac{2k\mu_1}{1+k} \left[\frac{y_1}{R_1^3} - \frac{a^2}{d^2} \frac{y_2}{R_2^3} \right], \tag{33}$$

where

$$\begin{aligned} R_2^2 &= r^2 + 2\frac{a^2}{d} r\cos\theta + \frac{a^4}{d^2}, \\ R_3^2 &= r^2 - 2\frac{a^2+cd}{c+d} r\cos\theta + \frac{(a^2+cd)^2}{(c+d)^2}, \\ R_4^2 &= r^2 - 2\frac{a^2(c+d)}{a^2+cd} r\cos\theta + \frac{a^4(c+d)^2}{(a^2+cd)^2}. \end{aligned} \tag{34}$$

The image system for a transverse dipole located on the conducting cylinder C_a side consists of dipoles of strengths

$$p_2 = -\mu_1 \frac{a^2}{d^2}, \qquad p_3 = \mu_1 \frac{(1-k)b^2}{(1+k)(c+d)^2}, \qquad p_4 = -\mu_1 \frac{(1-k)(ab)^2}{(1+k)(a^2+cd)^2}, \tag{35}$$

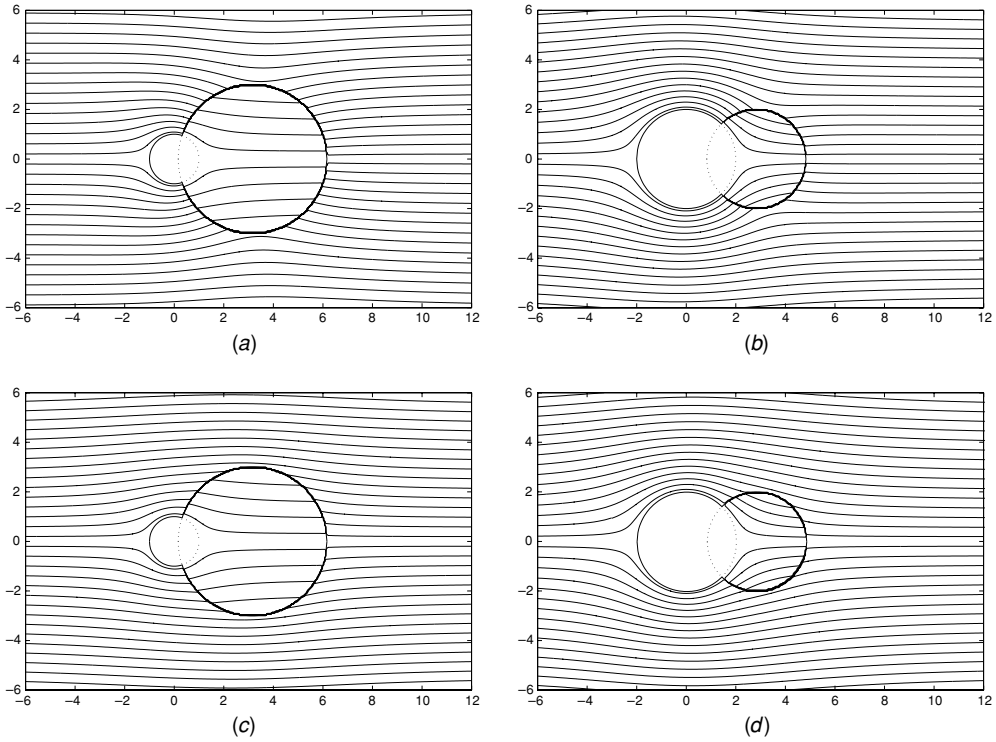

Figure 7. Equipotential plots for the uniform field along the longitudinal direction for different values of k and radii with $E = 1$. (i) $k = 0.5$: (*a*) $a = 1, b = 3$, (*b*) $a = 2, b = 2$; (ii) $k = 1.5$: (*c*) $a = 1, b = 3$, (*d*) $a = 2, b = 2$.

located at

$$D_2 = \left(-\frac{a^2}{d}, 0\right), \qquad D_3 = \left(-\frac{b^2}{c+d}, 0\right), \qquad D_3 = \left(-\frac{a(c+d)}{a^2+cd}, 0\right). \tag{36}$$

Note that the dipole strengths satisfy the following interesting relation:

$$\frac{1-k}{1+k}\frac{1}{p_2} + \frac{1}{p_3} = \frac{1-k}{1+k}\frac{1}{p_1} + \frac{1}{p_4}. \tag{37}$$

The above relation may have a physical significance which is an open question. A similar relation in the context of overlapping conducting spheres has been observed recently in [18]. It follows from (35) that the strengths of the image dipoles depend on the geometrical parameters, ratio of the two dielectric constants and the location of the initial dipole. The potentials in the two phases for a dipole located on the dielectric cylinder C_b side (that is located at $(c + d, 0)$, for instance) can be computed in the same manner.

Some representative potential plots for a single transverse dipole field in the presence of Γ for a fixed $k = k^{(\mathrm{I})}/k^{(\mathrm{II})}$ are portrayed in figures 8(*a*)–(*f*). The plots show some interesting patterns for the equipotentials. If the primary dipole (that is, the initial dipole in the absence of Γ) is located to the left of the conducting cylinder C_a, the equipotential curves in the dielectric phase II are straight for $b/a > 1$ as seen from figure 8(*a*). This pattern does not appear to change if the primary dipole is moved closer to the cylinder C_a (see figure 8(*b*)) keeping $b/a > 1$. However, for $b/a = 1$, the equipotentials display rather a different pattern in phase II as in figure 8(*c*). Some curves tend to bend towards the conducting

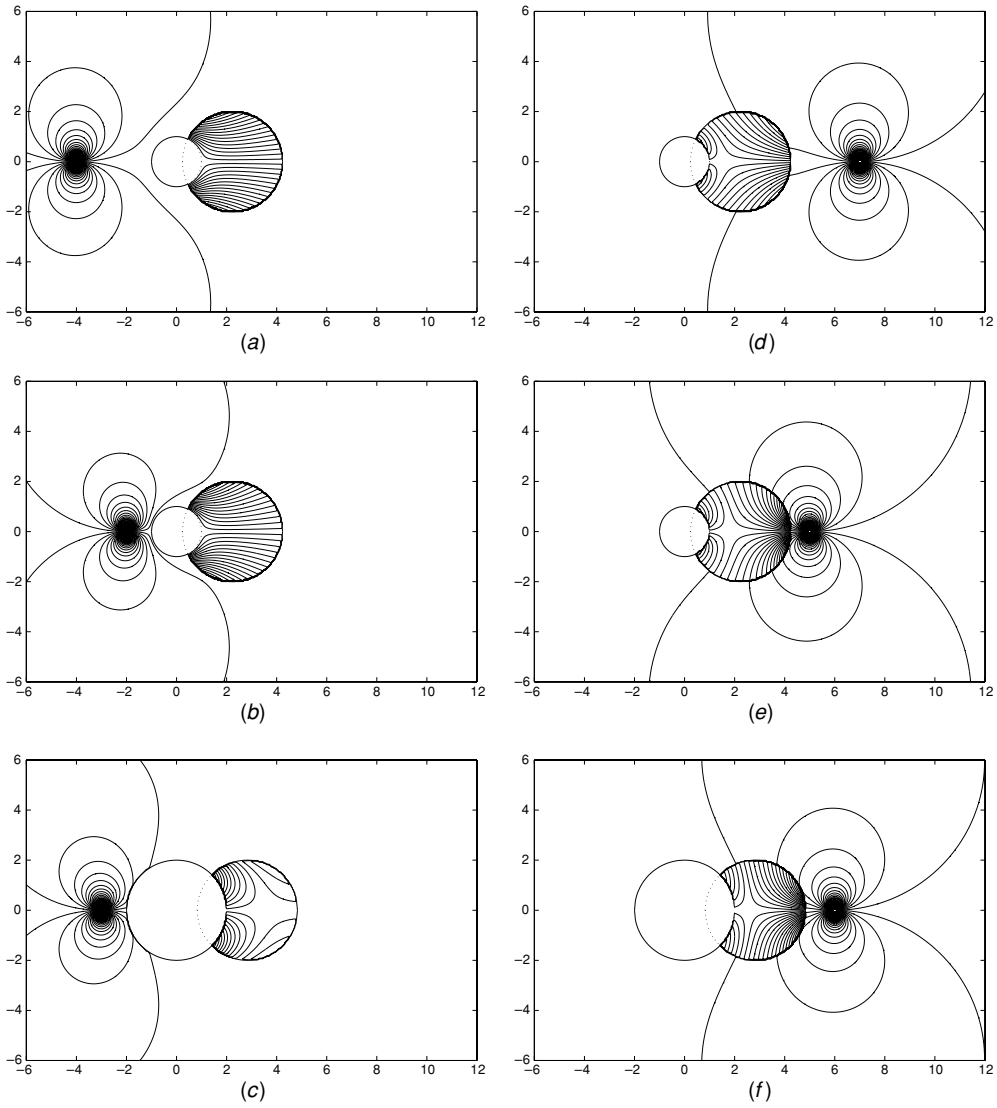

Figure 8. Equipotential plots for a single dipole field along the transverse direction for different locations for $k = 0.5$: (*a*) $a = 1, b = 2, d = a + 3$; (*b*) $a = 1, b = 2, d = a + 1$; (*c*) $a = 2, b = 2, d = a + 1$; (*d*) $a = 1, b = 2, d = c + 5$; (*e*) $a = 1, b = 2, d = c + 3$; (*f*) $a = 1, b = 2, d = c + 4$.

cylinder C_a in a symmetric fashion (symmetrical about the x-axis) and others pass straight through the dielectric cylinder C_b. It is fair to say that the radii ratio of the conducting and dielectric regions plays a crucial role in dictating the electric potential in phase II for a fixed k. Figures 8(*d*)–(*f*) display the equipotential patterns for a dipole located on the dielectric cylinder C_b side. The features of the equipotential curves in this case are qualitatively similar to that in figure 8(*c*). There is always a region in phase II where the lines bend towards the conductor C_a and this pattern continues to be the same for different radii ratios.

Figure 9 displays some representative equipotential curves generated by two similar transverse dipoles located on either side of Γ. When the two dipoles are situated at equidistance

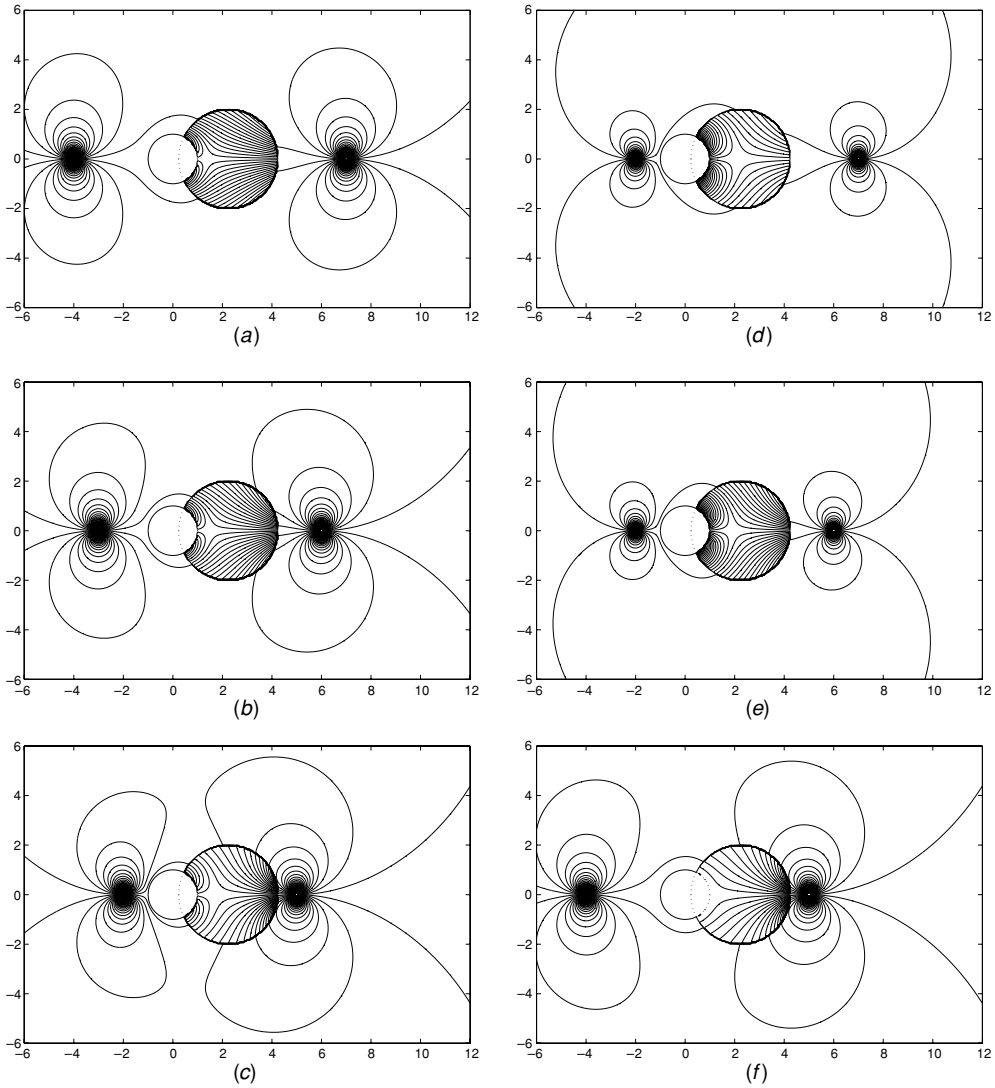

Figure 9. Equipotential plots for a pair of dipoles along the transverse direction for different locations with $k + 0.5, a = 1, b = 2$: (*a*) $d = a + 3, d_1 = c + 5$; (*b*) $d = a + 2, d_1 = c + 4$; (*c*) $d = a + 1, d_1 = c + 1$; (*d*) $d = a + 1, d_1 = c + 5$; (*e*) $d = a + 1, d_1 = c + 4$; (*f*) $d = a + 4, d_1 = c + 1$.

from each cylinder (i.e., $d = a + 3, d_1 = b + 3$), in phase II there is a smooth blending of the curves emanating from the initial dipoles (see figure 9(*a*)). The curves closer to the conducting cylinder bend towards it while the curves away from the conductor tend to become straight. This pattern remains the same even if the dipoles are moved closer to the cylinders C_a and C_b with the equidistant constraint as evident from figures 9(*b*) and 9(*c*). It is seen from figures 9(*c*)–(*e*) that the equipotential pattern continues to be the same even for non-equidistance locations of the primary dipoles. However, if the primary dipole on the dielectric cylinder side is closer to C_b and the other one on the conductor side is farther from C_a, then the potential pattern changes significantly. In fact, the equipotential curves tend to be stretched

along the diameter of cylinder C_b and there is no bending of curves towards the conductor C_a as seen in figure 9(f). To summarize, in the case of two initial dipoles located on either side of Γ, the location of the primary dipole on the dielectric cylinder side has potential significance on the equipotential patterns.

For the longitudinal dipole located outside Γ, the image system is found to have additional constants as explained in the case of longitudinal uniform field in subsection 5.1. The image system for other externally imposed potentials can be found in similar fashion using the general solutions (17) and (18).

6. Conclusion

Closed-form analytic solutions for the classical electrostatic problem involving a two-phase snowman-type geometry Γ consisting of two overlapping circles intersecting with a vertex angle $\pi/2$ are provided. Utilizing the image method, the general solutions for the electric potentials in both the phases are given in terms of the unbounded arbitrarily imposed potential in the form of a theorem followed by a simple proof. A connection of our results to the cyclic groups in abstract algebra is also provided in the appendix. The solutions to the related problems in electrostatics are also listed. The general solutions presented here are illustrated by numerous examples, namely (i) a two-phase object in a uniform field (both longitudinal and transverse fields) and (ii) a two-phase object embedded in a dipole field generated outside this geometry. The exact solutions in each case are interpreted in terms of the *Green* functions. In the case of uniform field, the dipole coefficients are extracted directly from the exact solutions. A nondimensional parameter connecting the dielectric constants of the two media is observed to play a crucial role. The other features including the equipotential plots are narrated in each example. The potential problems for other imposed fields in the presence of Γ can be treated in a similar manner.

We now have access to the solutions of Laplace equation for a new class of geometries. These solutions may be regarded as a set of basis for the method of reflections approach to compute many-body interactions in electrostatic and thermal environments. The documented preliminary results throw some light on development of image methods for non-circular hybrid geometries. The significant feature of this method, as evident from the present results, is that it avoids the use of a bicylindrical coordinate frame [14, 15]. It may be worthwhile to mention that the solutions for the two-dimensional problems have been obtained without recourse to conformal mapping techniques. This suggests that the results provided here may be utilized to solve boundary value problems involving complicated intersecting geometries by the use of möbius transformations. The possible generalizations of our results to pair of intersecting, dielectric particles in two and three dimensions including scalar transport problems [19] and bubbly flows [20] will be explored in the future. The connection between our solutions and abstract algebraic groups provided in the appendix is also clearly of interest.

Finally, the orthogonality condition that the two circles intersect at a vertex angle $\frac{\pi}{2}$ makes it possible to carry out a detailed analysis of the basic electrostatic problem for a nontrivial geometry. This critical assumption, even though a necessity to make analytical progress, is a first step towards solving the problem for arbitrary vertex angle, perhaps through some perturbation or numerical techniques. One of the advantages of this assumption is that it allows us to avoid the use of bicylindrical coordinates [14] to construct solutions of these problems which is very tedious and cumbersome. It is hoped that the technique presented here can be applied for the case when the two circles intersect at a vertex angle π/n, where n is an integer greater than 2. In such situations, the successive reflections will increase with increasing n, adding more number of terms to the general expressions for the electrostatic fields. However,

in the general case of arbitrary vertex contact angles, the problem has to be solved by the use of complicated functions in bicylindrical coordinates. It would certainly be interesting to analyse the influence of vertex angle on the electrostatic potentials and related physical quantities in the general case, but the possibility of solving such a problem still remains a challenge.

Acknowledgment

The author wishes to thank Professor Al Boggess, Head, Department of Mathematics, Texas A&M University, College Station, TX 77843, USA, for his help.

Appendix

There is a close connection between the general solutions given in equations (17) and (18) and the theory of cyclic groups [21, 22]. To see this connection, we define the operators L_a, L_b, $L_{ab} = L_{ba}$, M_b and M_{ab} in the following way:

$$L_a(\phi_0(x, y)) = -\phi_0\left(\frac{a^2}{r^2}x, \frac{a^2}{r^2}y\right), \tag{A.1}$$

$$L_b(\phi_0(x, y)) = -\frac{1-k}{1+k}\phi_0\left(c + \frac{b^2}{r'^2}x, \frac{b^2}{r'^2}y'\right), \tag{A.2}$$

$$L_{ab}(\phi_0(x, y)) = \frac{1-k}{1+k}\phi_0\left(\frac{a^2}{c} - \frac{a^2b^2}{c^2R^2}X, \frac{ab^2}{c^2R^2}Y\right), \tag{A.3}$$

$$M_b(\phi_0(x, y)) = \frac{2k}{1+k}\phi_0(x, y), \tag{A.4}$$

$$M_{ab}(\phi_0(x, y)) = -\frac{2k}{1+k}\phi_0\left(\frac{a^2}{r^2}x, \frac{a^2}{r^2}y\right). \tag{A.5}$$

Clearly, the operators L_a, L_b and L_{ab} correspond to inversions in the respective circles. Furthermore, these operators together with M_b and M_{ab} have the following properties:

- $L_a^2 = L_b^2 = I$, where I is the identity operator.
- $L_a(\phi_0(x, y))$, $L_b(\phi_0(x, y))$ and $L_{ab}(\phi_0(x, y))$ satisfy the same differential equation as ϕ_0 (that is, they satisfy the Laplace equation).
- $M_b(\phi_0(x, y))$ and $M_{ab}(\phi_0(x, y))$ also satisfy the Laplace equation.
- $(I + L_a + L_b + L_{ab})\phi_0(x, y)$ and $(M_b + M_{ab})\phi_0(x, y)$ satisfy the required boundary conditions on $\Gamma = C_a \cup C_b$.

Note that operator $L_{ab} = L_aL_b$ and that $L_aL_b = L_bL_a$ which means these two operators commute. We find that the set $G = \{I, L_a, L_b, L_{ab} = L_{ba}\}$ whose elements are operators occurring in the expressions (17) and (18), forms a group of order 4 (i.e., $o(G) = 4$) with composition as the group operation. Observe that G has a cyclic group C of order 2 whose elements are $C = \{I, L_{ab}\}$ and so $(L_aL_b)^2 = I$. It is interesting that the order of cyclic group is the same as the vertex angle in the present case. Perhaps this is true even in the general admissible case although the generalization may require further investigation.

References

[1] Thomson W (Lord Kelvin) 1845 Extrait D'une lettre de M. William Thomson a M. Liouville. Originally in *J. Math. Pures Appl.* **10** 364

Thomson W (Lord Kelvin) 1847 *J. Math. Pures Appl.* **12** 256–64
Thomson W (Lord Kelvin) 1872 *Electricity and Magnetism* (London: Macmillan) pp 144–6 (reprint)
[2] Maxwell J C 1954 *A Treatise on Electricity and Magnetism* (New York: Dover) chapter 11
[3] Smythe W R 1968 *Static and Dynamic Electricity* (New York: McGraw-Hill) chapter 4
[4] Binns K J and Lawrenson P J 1973 *Analysis and Computation of Electric and Magnetic Field Problems* (Oxford: Pergamon)
[5] Jones T B 1987 Effective dipole moment of intersecting conducting spheres *J. Appl. Phys.* **62** 362–5
[6] Milne-Thomson L M 1968 *Theoretical Hydrodynamics* (London: Macmillan)
[7] Lee D K 2000 Image singularity system to represent two circular cylinders of different diameter *Trans. ASME, J. Fluids Eng.* **122** 715–9
[8] Honein E, Honein T and Herrmann G 1992 On two circular inclusions in harmonic problems *Q. Appl. Math.* **50** 479–99
[9] Dassios G and Kleinmann R E 1989 On Kelvin inversion and low-frequency scattering *SIAM Rev.* **31** 565–85
[10] Van Bladel J 1968 Low frequency scattering by hard and soft bodies *J. Acoust. Soc. Am.* **44** 1069–73
[11] Power G 1953 A dielectric cylinder *Math. Gaz.* **37** 220
[12] Palaniappan D and Felderhof B U 1999 Electrostatics of the conducting double sphere *J. Appl. Phys.* **86** 3418–22
[13] Palaniappan D 2002 Electrostatics of two intersecting conducting cylinders *Math. Comput. Modelling* **36** 821–30
[14] Radchik A V, Smith G B and Reuben A J 1992 Quasistatic optical response of separate, touching, and intersecting cylinder pairs *Phys. Rev.* B **46** 6115–25
[15] Radchik A V, Paley A V, Smith G B and Vagov A V 1994 Polarization and resonant absorption of intersecting cylinders and spheres *J. Appl. Phys.* **76** 4827–35
[16] Haber S, Butler J P, Brenner H, Emanuel I and Tsuda A 2000 Shear flow over a self-similar expanding pulmonary alveolus during rhythmical breathing *J. Fluid Mech.* **405** 243–68
[17] Mansfield M L, Douglas J F and Garboczi E J 2001 Intrinsic viscosity and the electrical polarizability of arbitrarily shaped objects *Phys. Rev.* E **64** 061401
[18] Lindell I V, Wallen K H and Sihvola A H 2003 Electrostatic image theory for two intersecting conducting spheres *J. Electromagn. Wave* **17** 1643–60
[19] McPhedran R C, Poladian L and Milton G W 1988 Asymptotic studies of closely spaced, highly conducting cylinders *Proc. R. Soc. Lond.* A **415** 185–96
[20] Huang C, Lee J, Schultz W W and Ceccio S L 2003 Singularity image method for electrical impedance tomography of bubbly flows *Inverse Problems* **19** 919–31
[21] Ranger K B 1966 On the application of finite cyclic groups in potential theory *Proc. Lond. Math. Soc.* **16** 141–52
[22] Padmavathi B S, Raja Sekhar G P, Nigam S D and Amaranath T 2001 Group structure in circle theorem *Stud. Appl. Math.* **106** 407–17